LETTER

doi:10.1038/nature10347

Cell-to-cell spread of HIV permits ongoing replication despite antiretroviral therapy

Alex Sigal[1], Jocelyn T. Kim[1,2], Alejandro B. Balazs[1], Erez Dekel[3], Avi Mayo[3], Ron Milo[4] & David Baltimore[1]

Latency and ongoing replication[1] have both been proposed to explain the drug-insensitive human immunodeficiency virus (HIV) reservoir maintained during antiretroviral therapy. Here we explore a novel mechanism for ongoing HIV replication in the face of antiretroviral drugs. We propose a model whereby multiple infections[2,3] per cell lead to reduced sensitivity to drugs without requiring drug-resistant mutations, and experimentally validate the model using multiple infections per cell by cell-free HIV in the presence of the drug tenofovir. We then examine the drug sensitivity of cell-to-cell spread of HIV[4–7], a mode of HIV transmission that can lead to multiple infection events per target cell[8–10]. Infections originating from cell-free virus decrease strongly in the presence of antiretrovirals tenofovir and efavirenz whereas infections involving cell-to-cell spread are markedly less sensitive to the drugs. The reduction in sensitivity is sufficient to keep multiple rounds of infection from terminating in the presence of drugs. We examine replication from cell-to-cell spread in the presence of clinical drug concentrations using a stochastic infection model and find that replication is intermittent, without substantial accumulation of mutations. If cell-to-cell spread has the same properties *in vivo*, it may have adverse consequences for the immune system[11–13], lead to therapy failure in individuals with risk factors[14], and potentially contribute to viral persistence and hence be a barrier to curing HIV infection.

Current antiretroviral therapy (ART) does not cure HIV infection because low-level viraemia persists from virus reservoirs that are insensitive to ART[1]. The reservoirs may be long-lived infected cells, cells with latent virus, ongoing cycles of infection termed ongoing replication, or a combination of sources[1]. How ongoing replication might take place in the face of ART has remained unclear. If ART succeeds in decreasing ongoing HIV replication to very low levels, why does it not eliminate replication completely? Here we explore a novel mechanism for ongoing HIV replication in the presence of ART.

Multiple infections of one cell may propagate at drug concentrations where infection by single particles would die out: if more virions are transmitted per cell, the probability that at least one of the virions escapes the drug should increase (Fig. 1a). To model the effect of multiple infections on drug sensitivity (Supplementary Theory, section 1), we assume infections by individual virions are independent events, each with a probability of escaping the drug and succeeding in infecting the cell. To quantify infection sensitivity to drugs, we introduce the transmission index (T_X), which we define as the fraction of cells infected in the presence of drug (I_d) divided by the fraction of cells infected in the absence of drug (I). Given: (1) a multiplicity of infection of m infectious units per cell, where m is defined as the product of virus particle number and the probability of infection per virus particle; (2) a concentration of antiretroviral agent d that reduces m by factor $f(d)$, where $f(d) \geq 1$. Under these conditions, the transmission index is:

$$T_X = \frac{I_d}{I} = \frac{1-e^{-m/f(d)}}{1-e^{-m}} \quad (1)$$

T_X has two important limiting regimes: $m \ll 1$, in which case $T_X \approx 1/f(d)$ and $m/f(d) \gg 1$, in which case $T_X \approx 1$. In the first case, where few viruses infect each cell, the infection is sensitive to the effect of the drug, whereas in the second, where many viruses infect each cell, the infection is insensitive.

To test this, we infected the highly infection-permissive MT-4 T-cell line with cell-free HIV encoding yellow fluorescence protein (YFP)[15] at low (0.2) and high (100) m in the presence of tenofovir (TFV), a nucleotide reverse transcriptase inhibitor. We determined infected cell number by YFP fluorescence (Supplementary Fig. 1) and observed that infection with cell-free virus at low m was sensitive to TFV across the range of concentrations used. At high m, infection was insensitive to low and intermediate TFV concentrations (Fig. 1b), supporting the model. Thus, multiple cell-free HIV infections per cell recapitulate the insensitivity to drug of an HIV reservoir.

Multiple infections occur *in vivo*[2,16] and in culture[8,10] and are thought to be associated with cell-to-cell spread[2,8–10], a directed transmission mode that minimizes the number of virus particles failing to

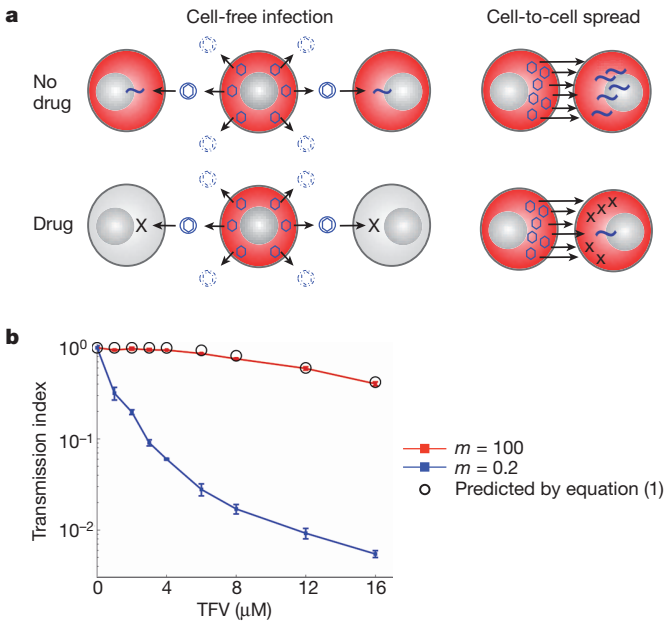

Figure 1 | Multiple infections per cell decrease sensitivity to drug. **a**, Hypothesis. Red circles indicate infected cells, arrows indicate transmissions, hexagons or hexagons surrounded by circles indicate viruses, broken circles indicate degraded viruses, crosses indicate viruses blocked by drug and wavelets indicate successful infection. **b**, MT-4 cells were pre-incubated with TFV and infected with HIV coding for YFP. Infection multiplicity m was 0.2 (blue squares) or 100 (red squares). Lines are a guide for the eye. Mean ± standard deviation (s.d.) of replicates ($n = 3$). Circles represent calculated values of T_X at $m = 100$ according to equation (1) with $f(d)$ at each drug concentration determined empirically at $m = 0.2$.

[1]Division of Biology, California Institute of Technology, Pasadena, California 91125, USA. [2]Division of Infectious Diseases, Department of Medicine, David Geffen School of Medicine at UCLA, Los Angeles, California 90095, USA. [3]Department of Molecular Cell Biology, Weizmann Institute of Science, Rehovot 76100, Israel. [4]Department of Plant Sciences, Weizmann Institute of Science, Rehovot 76100, Israel.

reach the target cell. We therefore used co-culture with infected cells to generate cell-to-cell spread and compared drug sensitivity to infection with cell-free virus. Infection by co-culture occurs both by cell-free virus shed by infected donor cells and by cell-to-cell spread. Administration of cell-free virus lacks a cell-to-cell component—the measured average virus cycle time (1.7 days; Supplementary Fig. 2) would rarely permit cell-free virus infected cells to complete a second round of infection during the experiment (2 days). Therefore, we compared cell-free virus infection and the combination of cell-free virus infection and cell-to-cell spread resulting from co-culture. We used drugs that act far downstream of entry, to ensure any differences between cell-to-cell and cell-free infection are not due to factors that physically inhibit drug action in cell-to-cell spread.

We infected peripheral blood mononuclear cells (PBMCs) in the presence or absence of TFV by co-culture or using cell-free virus. To separate donor from target cells in co-culture, we used HLA-A2-negative donor cells and HLA-A2-positive targets (Supplementary Fig. 3a). Two days post-infection, we determined the fraction of target cells infected using p24 intracellular staining of HLA-A2-positive PBMCs (Fig. 2a, top panel, controls in Supplementary Fig. 3b). Co-culture dramatically decreased sensitivity to drug: TFV decreased cell-free infection ~30-fold but caused less than a twofold decrease of co-culture infection (Fig. 2b). The decline in HLA-A2 expression in the target cells after infection (Supplementary Fig. 3b) is consistent with observations that productive HIV infection downregulates HLA[17].

We also used Rev-CEM[18] reporter T cells as targets. These cells express green fluorescent protein (GFP) in the presence of HIV early proteins Tat and Rev (Supplementary Fig. 4). To infect Rev-CEM cells, we used either cell-free HIV or co-culture with infected MT-4 cells engineered to be >99% mCherry positive (Supplementary Fig. 5). We excluded GFP/mCherry double-positive cells from the analysis to avoid scoring fused cells as infected (Supplementary Figs 6 and 7). This underestimates co-culture infection because it excludes unfused cell doublets in the process of virus exchange.

To block infection, we applied TFV and the non-nucleoside reverse transcriptase inhibitor efavirenz (EFV) (Fig. 2a, bottom panel, Supplementary Fig. 7). At the highest concentrations used, co-culture T_X was over sixfold higher than cell-free infection T_X (Fig. 2b). The trend was similar when donors were PBMCs or Rev-CEM cells (Supplementary Fig. 8). Co-culture T_X was lower than in PBMC-to-PBMC transmission, suggesting that target cells have an important role in cell-to-cell spread efficiency. The lower drug sensitivity in co-culture was not due to secreted donor cell factors that decrease the susceptibility of target cells to drugs (Supplementary Fig. 9).

We next determined the number of infectious units (m) transmitted. For co-culture, m was previously proposed to have a two-peaked Poisson distribution, one peak corresponding to cell-free virus or some low virus cell-to-cell transmissions, and the second to high virus number transmissions[3,9]. We fit a two-peaked Poisson and other distributions to the data (Supplementary Theory, section 2). The two-peaked Poisson fit the data best (Fig. 2b, dotted line, Supplementary Fig. 10). The first peak mean was ~1 infectious unit for both drugs, with 94% and 97% of infections in this peak for TFV and EFV, respectively. The second peak mean was 73 (TFV) and 175 (EFV), with the remaining 6% and 3% of infections in this peak. This predicts that whereas most infections are cell-free or low virus cell-to-cell transmissions, a minority involve very large numbers of viruses. This might seem to imply large numbers of integrations in the absence of drug in the high virus number subset. Arguing against this is our observation of a significantly increased cell death rate with increasing numbers of multiple infections in the absence of drugs (data not shown). Inter-virus interference, such as downregulation of CD4 receptors[19], may also limit provirus number.

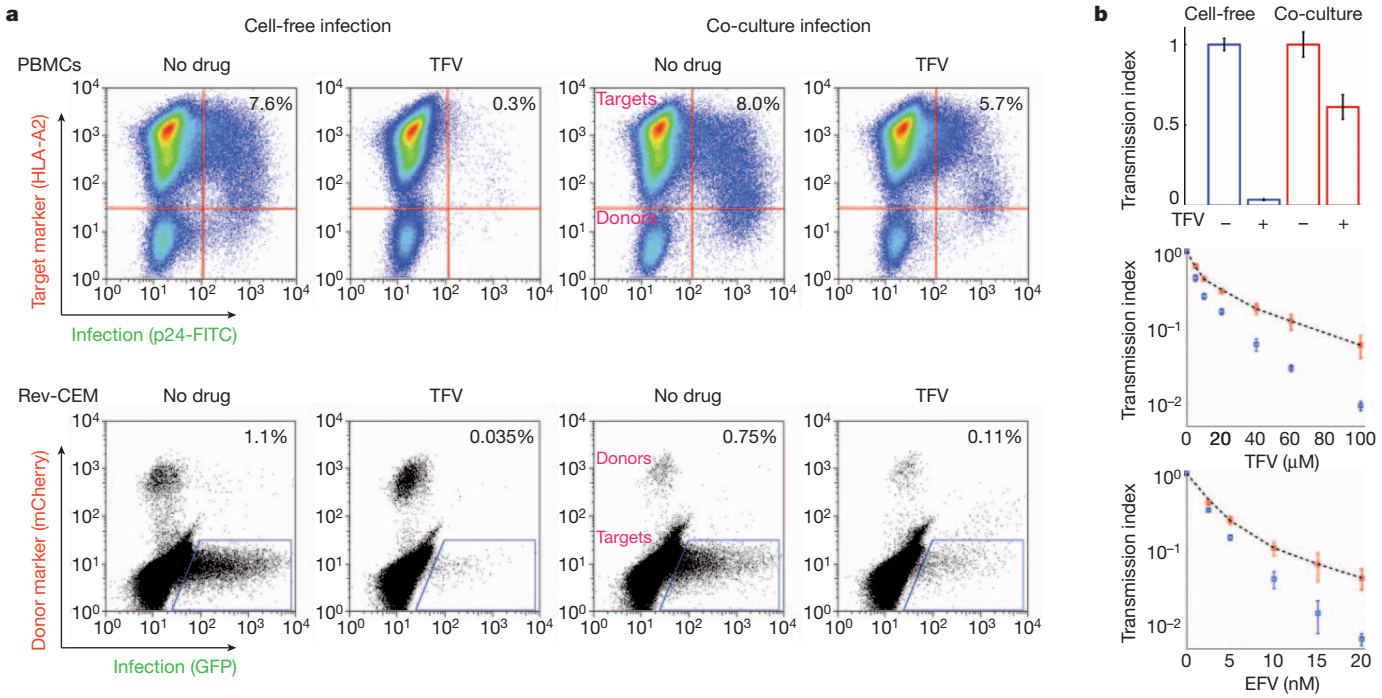

Figure 2 | Cell-to-cell spread reduces sensitivity to drugs. **a**, Top, infection of HLA-A2-positive PBMC targets with cell-free virus (left two plots) or infected HLA-A2-negative PBMC donors (right two plots) in the absence or presence of 10 μM TFV. x-axis is p24, y-axis HLA-A2 status. Bottom, the number of GFP-positive Rev-CEM cells after infection with cell-free virus (left two plots) or infected MT-4mCherry donors (right two plots) in the absence or presence of 60 μM TFV. x-axis is GFP, y-axis is mCherry fluorescence. **b**, Transmission index when infection source was cell-free HIV (blue bars or squares) or co-culture with HIV-infected donor cells (red bars or squares). Mean ± s.d. ($n = 3$). Top graph is PBMCs with TFV, middle graph is Rev-CEM cells with TFV, bottom graph is Rev-CEM cells with EFV. Black dashed line is best fit of m with a two-peaked Poisson distribution described by $p(m;a,\mu_1,\mu_2) = (1-a)e^{-\mu_1}\mu_1^m/m! + ae^{-\mu_2}\mu_2^m/m!$, where μ_1 and μ_2 are the means of the first and second peak respectively, and a is the fraction of transmissions that fall within the second peak. For TFV, $\mu_1 = 1.1$, $\mu_2 = 73$, $a = 0.06$. For EFV, $\mu_1 = 0.8$, $\mu_2 = 175$, with $a = 0.03$. Root mean squared error was 0.01 (EFV) to 0.02 (TFV).

To investigate whether cell-to-cell spread can lead to HIV replication through multiple virus cycles with ART, we measured the replication ratio (R), defined as fold change in the number of infected cells per virus cycle under conditions where target cells are not limiting: $(I_k/I_0)^{1/k}$. Here k is the number of elapsed virus cycles, I_k is the number of infected cells at virus cycle k, and I_0 is the number of infected cells at the start. For expanding infections $R > 1$, whereas infections with $R < 1$ ultimately terminate[20,21]. Although this assumes synchronized virus cycles, we simulated desynchronization and observed that its effect was negligible at the measured variability in cycle lengths (Supplementary Fig. 11).

To measure R, we tracked infection daily (Methods) in the absence of drug, with 100 μM TFV, or with a combination of EFV, TFV and the nucleoside reverse transcriptase inhibitor emtricitabine (FTC) at their clinical maximum plasma concentrations (C_{max}: 10 μM EFV, 2 μM TFV and 10 μM FTC[22]). The fraction of infected cells was kept low to ensure that target cells were not limiting. R_0, R_{TFV} and $R_{C_{max}}$, the replication ratios with no drug, TFV or at C_{max}, were fitted from the data (Fig. 3a, dashed lines). They were 65, 2.5 and 0.95, respectively. R_{TFV} was significantly greater than 1 ($P < 0.01$), indicating an expanding infection. $R_{C_{max}}$ was slightly lower than 1 in all experiments (Supplementary Fig. 12), indicating an infection slightly below the expansion threshold.

We compared experimentally obtained replication ratios with those predicted for the same drug concentrations if cell-free infection were the only infection route (Supplementary Theory section 3 and Supplementary Fig. 13). We obtained $R_{TFV} = 1.1$ and $R_{C_{max}} = 0.60$ values in this case (Fig. 3a). The predicted R with no replication, resulting solely from infected cell half-life, was 0.46 (Fig. 3a). Predicted cell-free replication ratios were significantly lower ($P < 0.02$ for TFV, $P < 0.01$ for C_{max}) than ratios experimentally obtained from co-culture.

Given the lack of evolution in the plasma in individuals with HIV successfully suppressed by drugs[23,24], ongoing replication can occur if: (1) it is compartmentalized to other locations[25,26], (2) if it is intermittent; (3) the circulating virus is at a fitness maximum[24]; or some combination of these factors. We obtained $R_{C_{max}} = 0.95$. If this is extrapolated *in vivo*, it follows that ongoing replication cannot persist independently but may have a role if it interacts with another reservoir that primes replication[27]. To examine this scenario, we performed a stochastic simulation (Methods). As expected for intermittent replication, every infection chain that starts from the introduction of an infected cell from a different reservoir—for example, reactivation from latency—terminates (Supplementary Fig. 14). A constant input of one infected cell per virus cycle results in a steady state where substantial numbers of newly infected cells are generated, but the average number of mutations anywhere on the HIV genome per infected cell is low (~1; Fig. 3b). Because each infection chain is independent, these mutations are expected to be sporadic and not linked by temporal structure.

Evidence for ongoing replication during ART derives from the decrease in virus decline rates[28], some HIV sequence divergence[29] and long terminal repeat circle formation when the integrase inhibitor raltegravir is included in drug regimens[11]. At least in some individuals, antiretroviral suppression is close to the ongoing replication threshold: a mutation conferring very low-level resistance to EFV at therapy initiation[30] is sufficient to cause ongoing replication, as indicated by increased virological failure risk[14]. Our data indicate that cell-to-cell spread is a likely source of intermittent ongoing replication in the face of ART, and that this is a consequence of some cell-to-cell infections transmitting virus numbers much in excess of what is required to infect a cell in the absence of ART. The large transmitted dose strongly decreases the probability that every transmitted virus will be inhibited by the drugs, and therefore greatly weakens their effect. This replication may adversely affect the immune system, increasing activation[11,12] and cell death[13], and could potentially contribute to the maintenance of an HIV reservoir in locations such as lymphoid tissue where cell-to-cell spread occurs.

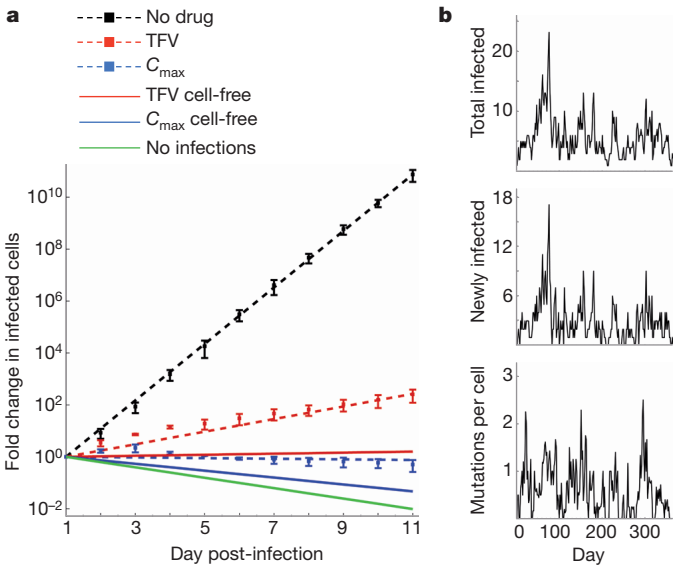

Figure 3 | Co-culture infection dynamics. **a**, Infection growth rate. Drug conditions were: no drug (black squares), 100 μM TFV (red squares) and C_{max} (blue squares). Means ± s.d. of inter-day experiments ($n = 3$). Dashed lines represent fits of $I_k = I_0 R^k$ for each drug condition. Solid lines are predicted infection dynamics for infection occurring exclusively by cell-free virus in the presence of 100 μM TFV (red line), C_{max} (blue line), or with no viral replication (green line). **b**, Simulation of the number of infected cells and mutations per cell with an input of one infected cell per virus cycle (Methods). x-axis is time, y-axis is number of total infected cells (top graph), newly infected cells (middle graph) or sum of mutations divided by the sum of total infected cells (bottom graph). Average number of mutations per cell over time is 0.6 ± 0.5 (mean ± s.d., $n = 215$).

METHODS SUMMARY

HIV infection at high and low *m*. NL4-3YFP HIV stock at a 1:2,000 or 1:4 final dilution was added to MT-4 cells pre-incubated with TFV. Two days post-infection, the number of YFP-positive cells was determined by FACS. The multiplicity of infection was calculated as $m = -\ln p(0) = -\ln(1 - I_{1:2,000})$, where $I_{1:2,000}$ is the fraction of YFP-positive cells at the 1:2,000 dilution.

Drug sensitivity of co-culture versus cell-free infections. Donor cells were infected with NL4-3 strain HIV and incubated for two to three days. Infected donor cells or cell-free NL4-3 were then added to target cells. Two days after target cell infection, the number of infected cells was determined by FACS using intracellular p24 staining (PBMCs) or GFP expression (Rev-CEM cells). In all experiments, uninfected PBMC or MT-4mCherry cells were added to cell-free virus infections to keep total cell numbers equal on day 0.

Infection growth rate. Infection was initiated by adding infected Rev-CEM cells to uninfected Rev-CEM cells pre-incubated with drugs. Cells were passaged on each day following infected cell addition: infection with no drug was split 1:10 into fresh Rev-CEM cells. For 100 μM TFV or C_{max}, infected cells were split 0.6:1 with drug-containing medium. Cells remaining after split were used to quantify the fraction of infected cells by FACS. The fold change in infected cells on each day was calculated as $N_k D_k / N_0$, where N_k is the fraction of infected cells on day k, D_k is total dilution factor (split) up to day k and N_0 is the fraction of infected cells on day 1.

Full Methods and any associated references are available in the online version of the paper at www.nature.com/nature.

Received 30 November 2010; accepted 1 July 2011.
Published online 17 August 2011.

1. Pierson, T., McArthur, J. & Siliciano, R. F. Reservoirs for HIV-1: mechanisms for viral persistence in the presence of antiviral immune responses and antiretroviral therapy. *Annu. Rev. Immunol.* **18,** 665–708 (2000).
2. Jung, A. *et al.* Recombination: multiply infected spleen cells in HIV patients. *Nature* **418,** 144 (2002).
3. Dixit, N. M. & Perelson, A. S. HIV dynamics with multiple infections of target cells. *Proc. Natl Acad. Sci. USA* **102,** 8198–8203 (2005).
4. Dimitrov, D. S. *et al.* Quantitation of human immunodeficiency virus type 1 infection kinetics. *J. Virol.* **67,** 2182–2190 (1993).

5. Sattentau, Q. Avoiding the void: cell-to-cell spread of human viruses. *Nature Rev. Microbiol.* **6,** 815–826 (2008).
6. Martin, N. *et al.* Virological synapse-mediated spread of human immunodeficiency virus type 1 between T cells is sensitive to entry inhibition. *J. Virol.* **84,** 3516–3527 (2010).
7. Sourisseau, M., Sol-Foulon, N., Porrot, F., Blanchet, F. & Schwartz, O. Inefficient human immunodeficiency virus replication in mobile lymphocytes. *J. Virol.* **81,** 1000–1012 (2007).
8. Dang, Q. *et al.* Nonrandom HIV-1 infection and double infection via direct and cell-mediated pathways. *Proc. Natl Acad. Sci. USA* **101,** 632–637 (2004).
9. Dixit, N. M. & Perelson, A. S. Multiplicity of human immunodeficiency virus infections in lymphoid tissue. *J. Virol.* **78,** 8942–8945 (2004).
10. Del Portillo, A. *et al.* Multiploid inheritance of HIV-1 during cell-to-cell infection. *J. Virol.* **85,** 7169–7176 (2011).
11. Buzón, M. J. *et al.* HIV-1 replication and immune dynamics are affected by raltegravir intensification of HAART-suppressed subjects. *Nature Med.* **16,** 460–465 (2010).
12. Chun, T. W. *et al.* Relationship between residual plasma viremia and the size of HIV proviral DNA reservoirs in infected individuals receiving effective antiretroviral therapy. *J. Infect. Dis.* **204,** 135–138 (2011).
13. Doitsh, G. *et al.* Abortive HIV infection mediates CD4 T cell depletion and inflammation in human lymphoid tissue. *Cell* **143,** 789–801 (2010).
14. Paredes, R. *et al.* Pre-existing minority drug-resistant HIV-1 variants, adherence, and risk of antiretroviral treatment failure. *J. Infect. Dis.* **201,** 662–671 (2010).
15. Levy, D. N., Aldrovandi, G. M., Kutsch, O. & Shaw, G. M. Dynamics of HIV-1 recombination in its natural target cells. *Proc. Natl Acad. Sci. USA* **101,** 4204–4209 (2004).
16. Gratton, S., Cheynier, R., Dumaurier, M. J., Oksenhendler, E. & Wain-Hobson, S. Highly restricted spread of HIV-1 and multiply infected cells within splenic germinal centers. *Proc. Natl Acad. Sci. USA* **97,** 14566–14571 (2000).
17. Collins, K. L., Chen, B. K., Kalams, S. A., Walker, B. D. & Baltimore, D. HIV-1 Nef protein protects infected primary cells against killing by cytotoxic T lymphocytes. *Nature* **391,** 397–401 (1998).
18. Wu, Y., Beddall, M. H. & Marsh, J. W. Rev-dependent indicator T cell line. *Curr. HIV Res.* **5,** 394–402 (2007).
19. Chen, B. K., Gandhi, R. T. & Baltimore, D. CD4 down-modulation during infection of human T cells with human immunodeficiency virus type 1 involves independent activities of vpu, env, and nef. *J. Virol.* **70,** 6044–6053 (1996).
20. Ribeiro, R. M. *et al.* Estimation of the initial viral growth rate and basic reproductive number during acute HIV-1 infection. *J. Virol.* **84,** 6096–6102 (2010).
21. Nowak, M. A. & May, R. M. *Virus Dynamics: Mathematical Principles of Immunology and Virology* (Oxford Univ. Press, 2000).
22. Mathias, A. A. *et al.* Bioequivalence of efavirenz/emtricitabine/tenofovir disoproxil fumarate single-tablet regimen. *J. Acquir. Immune Defic. Syndr.* **46,** 167–173 (2007).
23. Bailey, J. R. *et al.* Residual human immunodeficiency virus type 1 viremia in some patients on antiretroviral therapy is dominated by a small number of invariant clones rarely found in circulating $CD4^+$ T cells. *J. Virol.* **80,** 6441–6457 (2006).
24. Kieffer, T. L. *et al.* Genotypic analysis of HIV-1 drug resistance at the limit of detection: virus production without evolution in treated adults with undetectable HIV loads. *J. Infect. Dis.* **189,** 1452–1465 (2004).
25. Cu-Uvin, S. *et al.* Genital tract HIV-1 RNA shedding among women with below detectable plasma viral load. *AIDS* **24,** 2489–2497 (2010).
26. North, T. W. *et al.* Viral sanctuaries during highly active antiretroviral therapy in a nonhuman primate model for AIDS. *J. Virol.* **84,** 2913–2922 (2010).
27. Rong, L. & Perelson, A. S. Modeling latently infected cell activation: viral and latent reservoir persistence, and viral blips in HIV-infected patients on potent therapy. *PLOS Comput. Biol.* **5,** e1000533 (2009).
28. Grossman, Z. *et al.* Ongoing HIV dissemination during HAART. *Nature Med.* **5,** 1099–1104 (1999).
29. Frenkel, L. M. *et al.* Multiple viral genetic analyses detect low-level human immunodeficiency virus type 1 replication during effective highly active antiretroviral therapy. *J. Virol.* **77,** 5721–5730 (2003).
30. Rhee, S. Y. *et al.* Human immunodeficiency virus reverse transcriptase and protease sequence database. *Nucleic Acids Res.* **31,** 298–303 (2003).

Supplementary Information is linked to the online version of the paper at www.nature.com/nature.

Acknowledgements We thank B. K. Chen, A. Del Portillo, J. T. Schiffer, L. Corey, and G. Lustig for discussions. A.S. was supported by the Human Frontier Science Program Long Term Fellowship LT00946. J.T.K. was supported by the UCLA STAR fellowship and T32 AI089398. A.B.B. was supported by the amfAR Postdoctoral Research Fellowship 107756-47-RFVA. This work was supported by the Bill & Melinda Gates Foundation and by the National Institutes of Health (HHSN266200500035C) and a contract from the National Institute of Allergy and Infectious Diseases. We acknowledge the support of the UCLA CFAR Virology Core Lab (P01-AI-28697) and the UCSF-GIVI CFAR (P30-AI-27763).

Author Contributions A.S. and D.B. conceived the study. A.S. designed the research; A.S. and J.T.K. performed the experiments with support from A.B.B.; A.S. formulated the basic mathematical model and performed the numerical simulations; R.M., A.M. and E.D. added analytical insights and expanded the model to treat virus number as a random variable; A.S. and D.B. wrote the paper.

Author Information Reprints and permissions information is available at www.nature.com/reprints. The authors declare no competing financial interests. Readers are welcome to comment on the online version of this article at www.nature.com/nature. Correspondence and requests for materials should be addressed to D.B. (baltimo@caltech.edu).

METHODS

Cells, viruses and drugs. The following were obtained through the AIDS Research and Reference Reagent Program, National Institute of Allergy and Infectious Diseases, National Institutes of Health: Rev-CEM cells from Y. Wu and J. Marsh; MT-4 cells from D. Richman; HIV expression plasmid pNL4-3 from M. Martin; TFV; EFV. The NL4-3YFP molecular clone was a gift from D. Levy. Cell-free virus was produced by transfection of HEK293 cells with virus coding plasmid using Fugene 6 or Fugene HD (Roche). Supernatant containing shed virus was harvested after two days of incubation. Number of virus genomes of viral stock was determined using the RealTime HIV-1 Viral Load test (Abbott Diagnostics, Abbott Park Ill) and gag p24 content was determined by ELISA (Perkin-Elmer) at the the ARI-UCSF Laboratory of Clinical Virology. The MT-4mCherry cell line was created by infecting MT-4 cells with a pHAGE2 lentiviral vector expressing mCherry under the control of the EF1α promoter. To obtain a 0.99 fraction of mCherry-positive cells, MT-4mCherry cells were used fresh after lentiviral infection without a cycle of freezing and thawing, minimizing the number of population doublings and consequent decrease in the mCherry-positive fraction. Anonymous PBMCs or peripheral blood samples were provided by AllCells (PBMCs) or the UCLA Center for AIDS Research (CFAR) Virology Core Lab (peripheral blood). For whole blood, PBMCs were purified by Ficoll gradient using standard techniques. Purified PBMCs were activated with 5 μg ml^{-1} PHA in the presence of 5 ng ml^{-1} IL-2 for 1 (donors) or 3 (targets) days. All work was approved by the California Institute of Technology Institutional Biosafety Committee and Institutional Review Board exempt.

NL4-3YFP infection at high and low *m*. MT-4 cells were pre-incubated for 24 h with varying concentrations of TFV. NL4-3YFP stock was produced using transfection of HEK293 cells at 80% confluence with Fugene HD. Virus supernatant was collected 2 days post-transfection and added fresh to maximize the number of infectious units. Fresh virus stock was used at a 1:2,000 (low *m*) or 1:4 final dilution (high *m*). After 2 days incubation with virus, the number of YFP-positive MT-4 cells was quantified by flow cytometry by collecting 2×10^5 cells using a FACScaliber machine (Becton Dickenson). The multiplicity of infection was calculated using Poisson statistics: $m = -\ln p(0) = -\ln(1 - I_{1:2,000})$, where $p(0)$ is the fraction of YFP-negative cells, and $I_{1:2,000}$ is the fraction of YFP-positive cells at the 1:2,000 dilution.

Comparison of co-culture and cell-free infections in PBMCs. For PBMC infections, 1.5×10^6 PHA-activated HLA-A2-negative donor PBMCs at 10^6 cells ml^{-1} were either infected with 700 ng HIV (NL4-3 strain), or mock infected with the same volume of growth medium. Cells were then incubated for 2 days. Two days after donor-cell infection, PHA-activated HLA-A2-positive PBMC target cells at 10^6 cells ml^{-1} were either treated with no drug or 10 μM TFV. The stock of target cells with or without drug was then split into wells at 10^6 cells well^{-1} and incubated for 4 h. After target cell incubation, HLA-A2-negative donor PBMCs were washed, counted, diluted to 10^6 cells ml^{-1} and added to target cells at an approximately 1:10 donor:target ratio as follows. For cell-free infection, each well received 100 μl mock-infected HLA-A2-negative donor PBMCs and 150 μl (250 ng) cell-free NL4-3. For co-culture infection, each well received 100 μl infected HLA-A2-negative donor PBMCs and 150 μl growth medium. One day after target-cell infection, cell aggregates were broken up by repeated pipetting, and cells split 1:2 with fresh growth medium containing the corresponding drug concentration. Two days after target-cell infection, the number of infected target cells was determined: cells were stained with PE-conjugated anti-HLA-A2 antibody (BD Biosciences or Biolegend), fixed and permeabilized (Cytofix/cytoperm kit, BD Biosciences), then stained with intracellular FITC-conjugated anti-HIV p24 antibody (clone KC57, Coulter Corporation) according to the Cytofix/cytoperm kit protocol. The fraction of infected target cells was quantified by FACS as HLA-A2, p24 double-positive cells. We observed that PBMCs were infected best when fresh, and use of previously frozen material or cells whose processing was delayed substantially reduced both cell-free and co-culture infections.

Comparison of co-culture and cell-free infections using Rev-CEM cells. We infected Rev-CEM target cells either by co-culture with MT-4mCherry donor cells or cell-free virus. MT-4mCherry donor cells at 4×10^5 cells ml^{-1} were infected with 300 ng ml^{-1} p24 NL4-3, or mock infected with the same volume of growth medium. Donor cells were then incubated for 3 days. Two days after donor-cell infection and one day before target-cell infection, Rev-CEM target cells at 8×10^5 cells ml^{-1} were treated with no drug, TFV, or EFV. The stock of target cells with or without drug was then split into wells at 1.6×10^6 cells well^{-1} and incubated for 24 h. Three days after donor-cell infection, MT-4mCherry donor cells were washed, counted, diluted to 3×10^5 cells ml^{-1} and added at an approximately 1:100 donor:target ratio as follows. For cell-free infection, each well received 100 μl mock-infected MT-4mCherry donor cells and 600 μl (1 μg) cell-free NL4-3. For co-culture infection, each well received 100 μl infected MT-4mCherry donor cells and 600 μl growth medium. One day after target-cell infection, cell aggregates were broken up by repeated pipetting, and cells split 1:2 with fresh growth medium containing the corresponding drug concentration. Two days after target-cell infection, the number of infected target cells were quantified by FACS by mCherry and GFP fluorescence. Infected target cells were gated as positive for GFP, and negative for mCherry, thereby excluding uninfected Rev-CEM cells (GFP negative), MT-4mCherry cells (GFP negative, mCherry positive), and fusions between MT-4mCherry and Rev-CEM cells (GFP positive, mCherry positive). The fraction of MT-4mCherry donors was 1% on day 0 for both mock-infected and infected cells, but decreased for infected MT-4mCherry cells by the end of the target-cell infection, probably owing to the cytotoxicity of infection. To ensure that the low numbers of infected target cells gave repeatable results, we averaged consecutive independent inter-day experiments.

Infection growth rate. To initiate infection, Rev-CEM cells at 4×10^5 cells ml^{-1} were infected with 300 ng ml^{-1} NL4-3 in the absence of drugs and incubated for three days. Two days post-infection, uninfected Rev-CEM cells at 8×10^5 cells ml^{-1} were pre-treated with no drug, 100 μM TFV, or a combination of EFV, TFV and FTC at their clinical maximum plasma concentrations (C_{max}: 10 μM EFV, 2 μM TFV and 10 μM FTC). Three days after the initial infection with cell-free virus, the infected Rev-CEM cells were washed and added to a final fraction of 0.2% GFP-expressing donor cells to the uninfected Rev-CEM cells incubated with no drug, TFV or C_{max}. On each day after infected donor addition, cell aggregates were broken up by gentle repeated pipetting and cells split. Infection conditions were calibrated so that the number of uninfected target cells would not be limiting and infection would not interfere with proliferation of uninfected cells. Infection was therefore kept below ~0.5% GFP-expressing infected Rev-CEM cells. The daily cell dilution was calibrated to keep this steady state of infected cells: the sample with no drug was split 1:10 or 1:20 into fresh Rev-CEM cells in a new well. For 100 μM TFV or C_{max} drug concentrations, infected cells were split 0.6:1 with drug-containing medium into a new well. Cells remaining after cell split were used to quantify the fraction of infected cells by FACS (5×10^5 collected per sample). The fold change in infected cells on each day was calculated as $N_k D_k / N_0$, where N_k is the fraction of infected cells on day k, D_k is the total dilution factor up to day k and N_0 is the fraction of infected cells on day 1. The drug effect on a single round of cell-free infection for 100 μM TFV or C_{max} was measured at the same time as the infection growth rate to prevent differences in drug stock batch or cells.

Stochastic simulation of the number of infected cells and mutations. The purpose of the simulation was to determine the sum of total infected cells, newly infected cells, and mutations at each virus cycle (measured as 1.7 days (Supplementary Fig. 2)) from overlapping infection chains. A new infection chain was initiated each virus cycle with an input of one infected cell. The number of infected cells in cycle $k+1$ generated by infected cell j in cycle k was an integer ${I_{k+1}}^j = x_1 + x_2$, where x_1 was a random number from a Poisson distribution with an average μ_1 defined by the measured infected-cell half-life $\mu_1 = 2^{-\tau/t1/2} = 0.46$ (Supplementary Fig. 13 and Supplementary Theory, section 3), and x_2 was a random number from a Poisson distribution with an average μ_2 defined by $\mu_2 = R_{C_{max}} - \mu_1 = 0.49$ (Supplementary Theory, section 3). Given an outcome of N infected cells in cycle k, the number of total infected cells in virus cycle $k+1$ in the infection chain was $\sum_1^N (x_1^j + x_2^j)$, of which the number of newly infected cells was $\sum_1^N x_2^j$. A new infection chain from an input of one infected cell was generated every virus cycle. Therefore, infection chains overlapped, and the total output number of infected cells in virus cycle $k+1$ was a sum of infected cells at that virus cycle from all M infection chains: $\sum_1^M \sum_1^N (x_1^j + x_2^j)$. The number of newly infected cells was $\sum_1^M \sum_1^N x_2^j$. If a new infection occurred, the probability of mutation occurring at any one of the 10^4 nucleotides of the HIV genome was $1 - (1 - 3.4 \times 10^{-5})^{10^4} = 0.29$, where 3.4×10^{-5} is the per-base probability of mutation for the HIV reverse transcriptase, and $(1 - 3.4 \times 10^{-5})^{10^4}$ is the probability that no mutations occur during a single reverse transcription event. As a simplifying assumption, no fitness benefit or cost was assigned to individual mutations. Therefore, $R_{C_{max}}$ did not change during the course of the simulation. Surviving cells carried over their mutations to the next generation, and newly infected cells carried over mutations from the infected donor cells, in addition to any mutations generated during the infection process.